Controlling optical bistability in two-coupled quantum wells

CHUNCHAO YU[a,b,*], FANG CHEN[a,b], LIHUI SUN[a,b], HUAFENG ZHANG[a,b]
[a]*School of Physics and Optoelectronic Engineering, Yangtze University, Jingzhou, 434023, China*
[b]*Institute of Quantum Optics and Information Photonics, Yangtze University, Jingzhou, 434023, China*

The optical bistability (OB) is investigated theoretically in a unidirectional ring cavity containing two-coupled four-level quantum wells (QWs). Manipulating the field, frequency detuning, and the relative phase of the applied fields, can be used to control the OB behaviors. Such a structure may be more practical than those atomic ones because of its more flexible and adjustable properties. The results maybe used to optimize the optical switching design.

(Received October 4, 2018; accepted April 8, 2019)

Keywords: Optical bistability, Quantum well, Optical switching

1. Introduction

OB, based on quantum coherence, is very attractive and practical in the nonlinear optics, for it can be used in many aspects such as optical memories, switches, and logical gates and so on. So, in the first, many approaches have been used to realize OB in the atomic systems theoretically and experimentally [1-19], such as the spontaneously generated coherence, the applying of a low frequency driving field, the phase alteration, etc. For example, Chen et al. [17] reported OB due to two-photon absorption and cross Kerr nonlinearity in a four-level N-type atomic system. Hu et al. [19] studied OB in a tripod four-level atomic system through changing the intensity of the microwave field and the relative phase of the driven fields.

In the same time, many studies have also been carried out on the OB in the semiconductor QWs and quantum dots (QDs) [20-38], because there is much inherent superiority such as the great flexibilities in devices, the high nonlinear, large electric dipole moments and so on. For example, Karabulut et al. [21] investigated OB obtained by changing the electron sheet density and the intensity of the optical radiation in a symmetric QW. Li et al. [24] proposed OB oranges from tunneling coupling in an asymmetric double QW structure. Tian et al. [31] studied OB by double tunneling coupling in linear triple QD molecules. Asadpour et al. [34] reported optical bistability and multistability in QW controlled by biexciton energy renormalization due to many-particle coulomb interactions. Hamedi et al. [38] researched OB controlled by the tunneling coupling in a multifold QD molecule containing five QDs.

In this paper, we suggest two-coupled QWs to control the OB by second harmonic coupling field and another coupling fields via arranging carefully the corresponding parameters. In our proposal, different types of OB are controlled two-color coherently and researched theoretically.

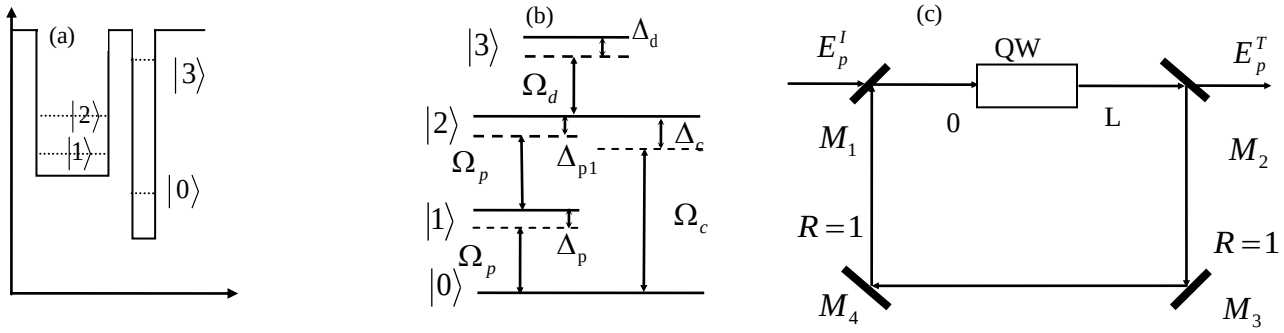

Fig. 1. QWs schematic diagram, the system energy levels and unidirectional ring cavity. (a) QWs contain four energy levels. (b) QWs system interacting with a probe and two coupling optical fields. (c) A unidirectional ring cavity contains QWs sample and four mirrors. E_p^I *(*E_p^T*) is the incident (transmitted) field*

2. Model and theory

We consider symmetric InGaAs/AlInAs double coupling QWs which can also be seen in [27] shown in Fig. 1 (a). It can be grown by Molecular Beam Epitaxy and has been used widely in modern solid state physics. $In_{0.47}Ga_{0.53}As$ with thin energy bandgap is sandwiched between $Al_{0.48}In_{0.52}As$ with wider bandgap on a lattice-matched undoped InP substrate. We can model the InGaAs/AlInAs QW and engineer it with our desired combination of properties. Under the effective mass approximation, we can solve the Schrödinger equation numerically and get the eigen energy and the Bolch wave functions. So we have designed the sample to have desired transition energy level in the range of 120-170 meV and dipole moments [27, 35, 39, 40]. Especially, the transition energy $|1\rangle \leftrightarrow |0\rangle$ and $|2\rangle \leftrightarrow |1\rangle$ can be designed to be similar for the probe laser. A coupling laser with Rabi frequency Ω_c (Ω_d) is mediated to the transition $|2\rangle \leftrightarrow |0\rangle$ ($|3\rangle \leftrightarrow |2\rangle$) shown in Fig. 1 (b). Assuming $\hbar = 1$ and in the interaction picture, the system Hamiltonian can be written as follows,

$$H_{\text{int}}^{I} = \begin{pmatrix} 0 & -\Omega_p e^{i\phi_p} & -\Omega_c e^{i\phi_c} & 0 \\ -\Omega_p e^{-i\phi_p} & \Delta_p & -\Omega_p e^{i\phi_p} & 0 \\ -\Omega_c e^{-i\phi_c} & -\Omega_p e^{-i\phi_p} & \Delta_c & -\Omega_d \\ 0 & 0 & -\Omega_d & \Delta_c + \Delta_d \end{pmatrix}, \quad (1)$$

where $\Omega_p = \mu E_p$ is the Rabi frequency of the probe laser field. $\Omega_c = \mu E_c$ and $\Omega_d = \mu E_d$ are the Rabi frequency of two coupling laser fields. In which, with minor error, we assume $\mu = \mu_{10} = \mu_{21} = \mu_{20} = \mu_{32}$ simply and μ_{ij} is the electric dipole moment of transition between $|i\rangle$ and $|j\rangle$. φ_p and φ_c are the initial phase of the probe and coupling field respectively. $\Delta_c = \omega_{20} - \omega_c$ and $\Delta_d = \omega_{32} - \omega_d$ are the detuning of the two coupling laser fields. $\Delta_p = \omega_{10} - \omega_p$ and $\Delta_{p1} = \omega_{21} - \omega_p$ are the detuning of the probe laser field shown in Fig. 1 (b). ω_{ij} is the transition frequency of the state $|i\rangle$ and $|j\rangle$. $\omega_{20} = \omega_{21} + \omega_{10}$, $\omega_c = 2\omega_p$, and $\Delta_c = \Delta_p + \Delta_{p1}$ are satisfied.

Substituting the system quantum state $\Psi(t) = a_0|0\rangle + a_1 e^{i\phi_p}|1\rangle + a_2 e^{i\phi_c}|2\rangle + a_3 e^{i\phi_c}|3\rangle$, with $a_j (j = 0-3)$ being the probability of the state $|j\rangle$, into the Schrödinger equation, we can obtain,

$$i\frac{d}{dt}a_0 = -\Omega_p a_1 - \Omega_c a_2, \quad (2a)$$

$$i\frac{d}{dt}a_1 = (\Delta_p - i\gamma_1)a_1 - \Omega_p a_0 - \Omega_p e^{i\phi} a_2, \quad (2b)$$

$$i\frac{d}{dt}a_2 = (\Delta_c - i\gamma_2)a_2 - \Omega_c a_0 - \Omega_p e^{-i\phi} a_1 - \Omega_d a_3, \quad (2c)$$

$$i\frac{d}{dt}a_3 = (\Delta_c + \Delta_d - i\gamma_3)a_3 - \Omega_d a_2, \quad (2d)$$

$$|a_1|^2 + |a_2|^2 + |a_3|^2 + |a_4|^2 = 1, \quad (2e)$$

where $\gamma_i (i = 1\text{-}3)$, the total decay rate , are added phenomenologically in Eq. (2). $\phi = \phi_c - 2\phi_p$ is the relative phase of the applied fields.

Solve Eq. (2) in the steady state [31], we can get

$$\rho_{10} = a_1 a_0^* = \frac{B}{A} \cdot \frac{|A|^2}{|A|^2 + |B|^2 + |D|^2 + |E|^2}, \quad (3)$$

$$\rho_{21} = a_2 a_1^* = \frac{D \cdot B^*}{|A|^2 + |B|^2 + |D|^2 + |E|^2}, \quad (4)$$

where,

$$A = \Gamma_1\Gamma_2\Gamma_3 - \Omega_p^2\Gamma_3 - \Omega_d^2\Gamma_1,$$

$$B = \Omega_p(\Omega_c\Gamma_3 e^{i\phi} + \Gamma_2\Gamma_3 - \Omega_d^2),$$

$$D = \Omega_c\Gamma_1\Gamma_3 + \Omega_p^2\Gamma_3 e^{-i\phi}, E = \Omega_d(\Omega_c\Gamma_1 + \Omega_p^2 e^{-i\phi}),$$

$$\Gamma_1 = \Delta_p - i\gamma_1, \Gamma_2 = \Delta_c - i\gamma_2, \Gamma_3 = \Delta_c + \Delta_d - i\gamma_3.$$

Now, the QWs sample of length L is put into in a unidirectional cavity (see Fig. 1(c)). For mirrors M_1 and M_2, $R+T=1$ and R (T) is the reflection (transmission) coefficient. Mirrors M_3 and M_4 have 100% reflectivity. Then, using the Maxwell's equation under the slowly envelope approximation, the dynamics of the probe field is studied. Considering the boundary conditions in the steady state, we can finally obtain [32],

$$\frac{\partial E_p}{\partial z} = iN\frac{\omega_p\mu}{2c\varepsilon_0}(\rho_{10} + \rho_{21}), \quad (5a)$$

$$E_p(0) = \sqrt{T}E_p^I + RE_p(L), \quad (5b)$$

$$E_p(L) = E_p^T/\sqrt{T}, \quad (5c)$$

with c being the light speed in the vacuum and N being the electronic number density. $RE_p(L)$ in Eq. (5b) describes a feedback mechanism of the mirrors.

In the mean-field limit, through $x = \mu E_P^T/\hbar\sqrt{T}$ and $y = \mu E_P^I/\hbar\sqrt{T}$, we can normalize the fields, and obtain the input-output relationship from Eq. (5),

$$y = x - iC(\rho_{10} + \rho_{21}), \quad (6)$$

with $C = N\omega_p L|\mu|^2/(2\hbar c\varepsilon_0 T)$ being the electronic cooperation parameter.

3. Numerical results

Now, we study theoretically the output field versus the input field in the steady state for different parameters shown in Figs. 2-8. For simplicity, the parameters are selected dimensionless by scaling γ = 1 meV.

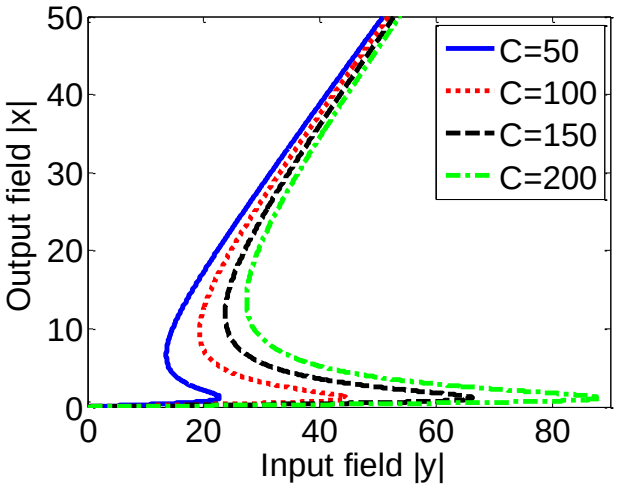

Fig. 2. Dependence of OB behavior on the electronic cooperation parameter C. The other used parameters are $\Omega_c=\Omega_d=1$, $\Delta_p=\Delta_c=\Delta_d=0$, $\phi=0$

First, Fig. 2 shows the dependence of OB behavior on the electronic cooperation parameter *C*. With the increasing of *C*, the threshold becomes larger due to $C \propto N$ for $C = N\omega_p L|\mu|^2/(2\hbar c\varepsilon_0 T)$.

Second, Fig. 3 shows the dependence of both OB and $\mathrm{Im}(\rho_{10}+\rho_{21})$ on the coupling frequency detuning Δ_c. In Fig. 3 (a), we can easily find, when Δ_c goes up, the OB threshold goes down. The reason can be found in Fig. 2 (b), the absorption $\mathrm{Im}(\rho_{10}+\rho_{21})$ goes down with the increasing of Δ_c, which means absorption weakening and accounts for decreasing in number of the OB threshold.

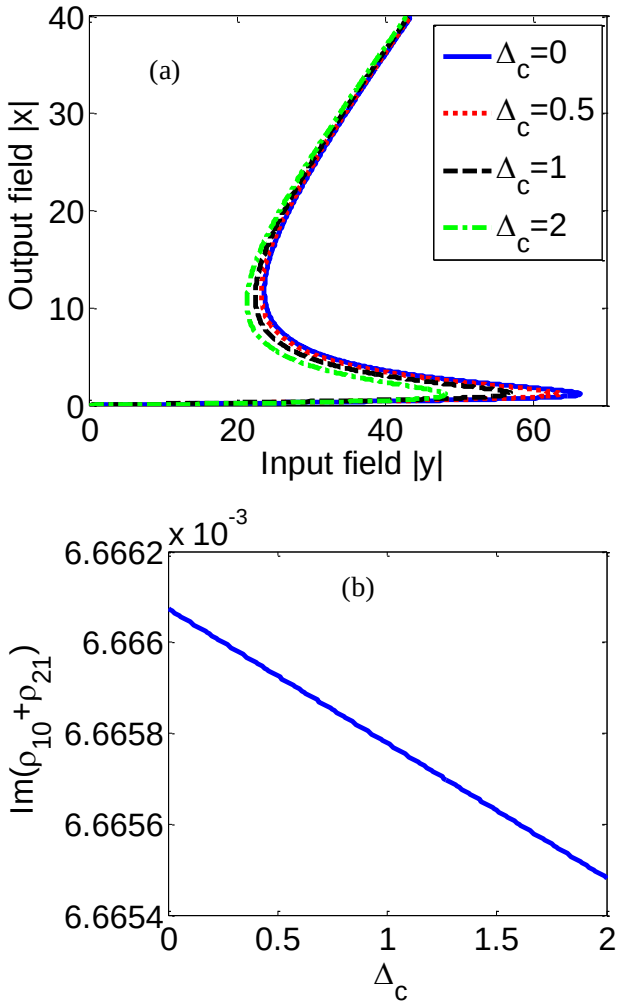

Fig. 3. Dependence of both OB and Im($\rho_{10}+\rho_{21}$) on the coupling-c frequency detuning Δ_c. (a) OB behavior for different values of Δ_c. (b) Im($\rho_{10}+\rho_{21}$) as a function of Δ_c with Ω_p=150. The other used parameters are, $\Omega_c=\Omega_d$=1, $\Delta_p=\Delta_d$=0, C=150, ϕ=0

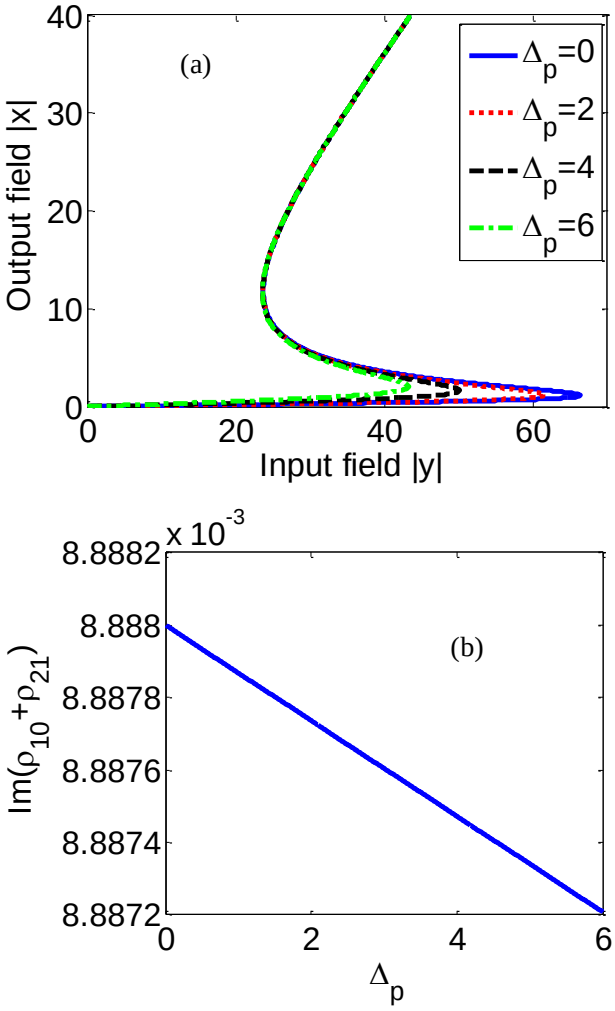

Fig. 4. Dependence of both OB and Im($\rho_{10}+\rho_{21}$) on the probing frequency detuning Δ_p. (a) OB behavior for different values of Δ_p. (b) Im($\rho_{10}+\rho_{21}$) as a function of Δ_p with Ω_p=150. The other used parameters are $\Omega_c=\Omega_d$=1, $\Delta_c=\Delta_d$= 0, C=150, ϕ=0

Third, Fig. 4 shows the dependence of both OB and Im($\rho_{10}+\rho_{21}$) on the probing frequency detuning Δ_p. Obviously, the OB threshold goes down with the increasing of the probing frequency detuning Δ_p in Fig. 4 (a). It is because the absorption Im($\rho_{10}+\rho_{21}$) decreases with the increasing of the probing frequency detuning Δ_p in Fig. 4 (b).

Fourth, Fig. 5 shows the dependence of both OB and Im($\rho_{10}+\rho_{21}$) on the coupling frequency detuning Δ_d. It is easy to see, with the increasing of the Δ_d, OB threshold goes down in Fig. 5 (a) due to the decreasing of the absorption Im($\rho_{10}+\rho_{21}$) in Fig. 5 (b).

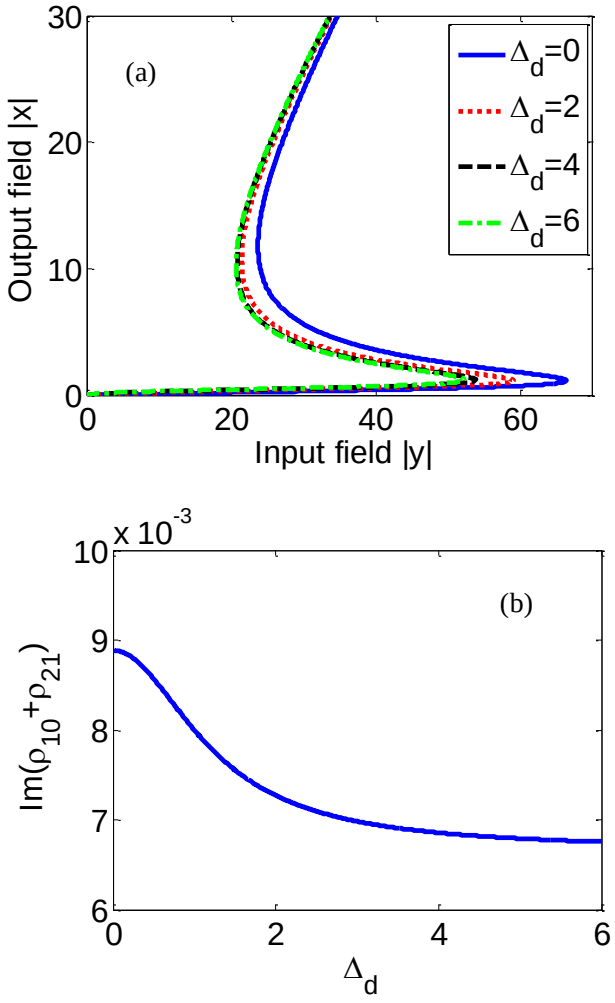

Fig. 5. Dependence of both OB and Im($\rho_{10}+\rho_{21}$) on the coupling frequency detuning Δ_d. (a) OB behavior for different values of Δ_d. (b) Im($\rho_{10}+\rho_{21}$) as a function of Δ_d with Ω_p=150. The other used parameters are, $\Omega_c=\Omega_d$=1, $\Delta_p=\Delta_c$=0, C=150, ϕ=0

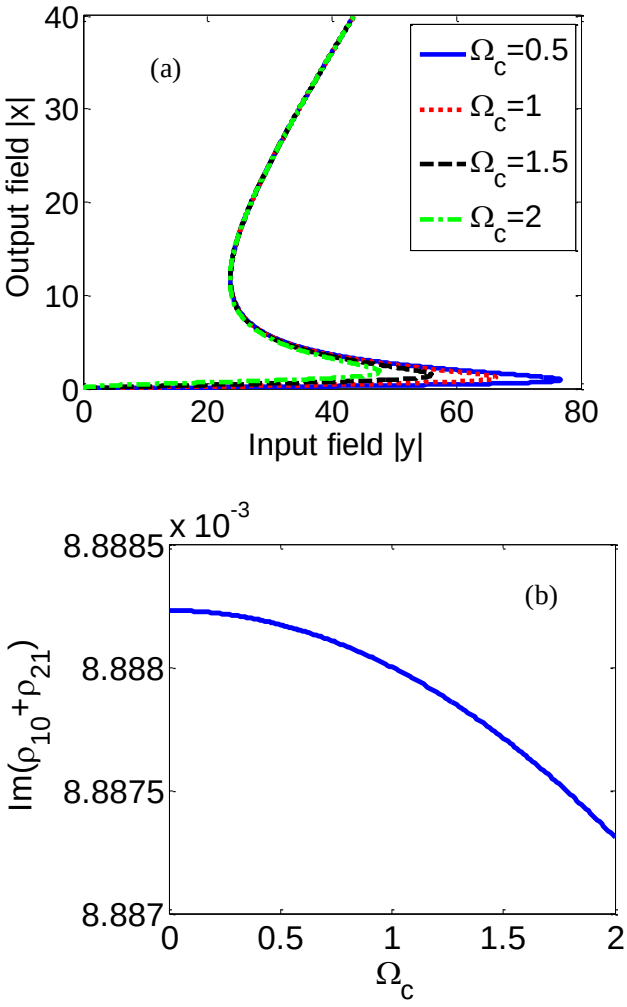

Fig. 6. Dependence of both OB and Im($\rho_{10}+\rho_{21}$) on the coupling-c field. (a) OB behavior for different values of Ω_c. (b) Im($\rho_{10}+\rho_{21}$) as a function of Ω_c with Ω_p=150. The other used parameters are $\Delta_p=\Delta_c=\Delta_d$=0, Ω_d=1, C=150, ϕ=0

Fifth, Fig. 6 shows the dependence of both OB and Im($\rho_{10}+\rho_{21}$) on the coupling-c (the field subscript being c) laser field. When the coupling-c field is enhanced, the threshold of OB reduces in Fig. 6 (a) due to the absorption Im($\rho_{10}+\rho_{21}$) decreasing in Fig. 6 (b).

Sixth, Fig. 7 shows the dependence of both OB and Im($\rho_{10}+\rho_{21}$) on the coupling-d (the field subscript being d) laser field. When the coupling-d field is enhanced, the threshold of OB goes up in Fig. 6 (a) for the absorption Im($\rho_{10}+\rho_{21}$) increasing in Fig. 7 (b).

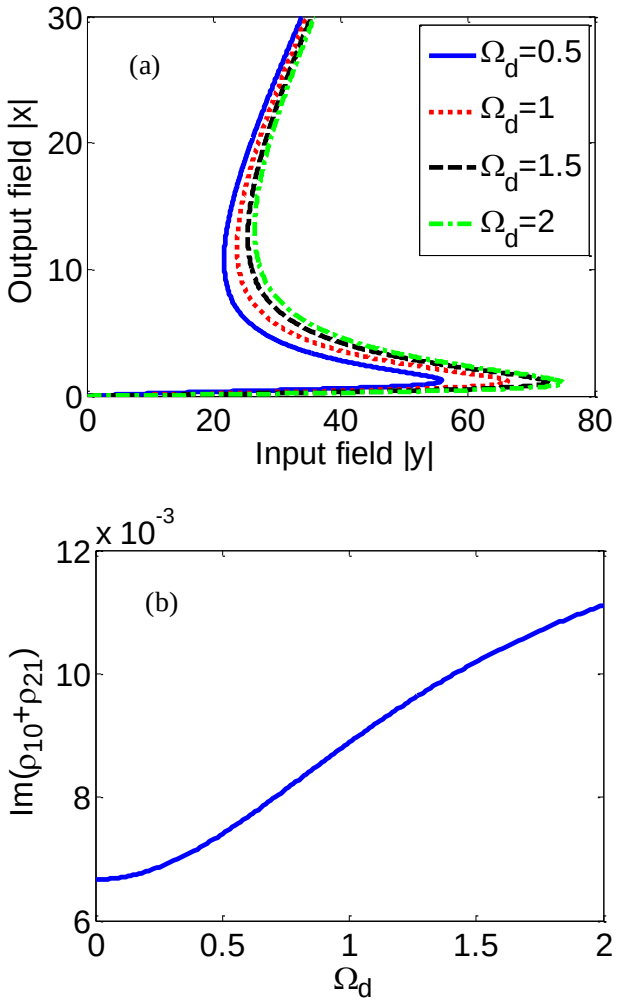

Fig. 7. Dependence of both OB and Im($\rho_{10}+\rho_{21}$) on the coupling-d field. (a) OB behavior for different values of Ω_d. (b) Im($\rho_{10}+\rho_{21}$) as a function of Ω_d with Ω_p=150. The other used parameters are $\Delta_p=\Delta_c=\Delta_d=0$, Ω_c=1, C=150, ϕ=0

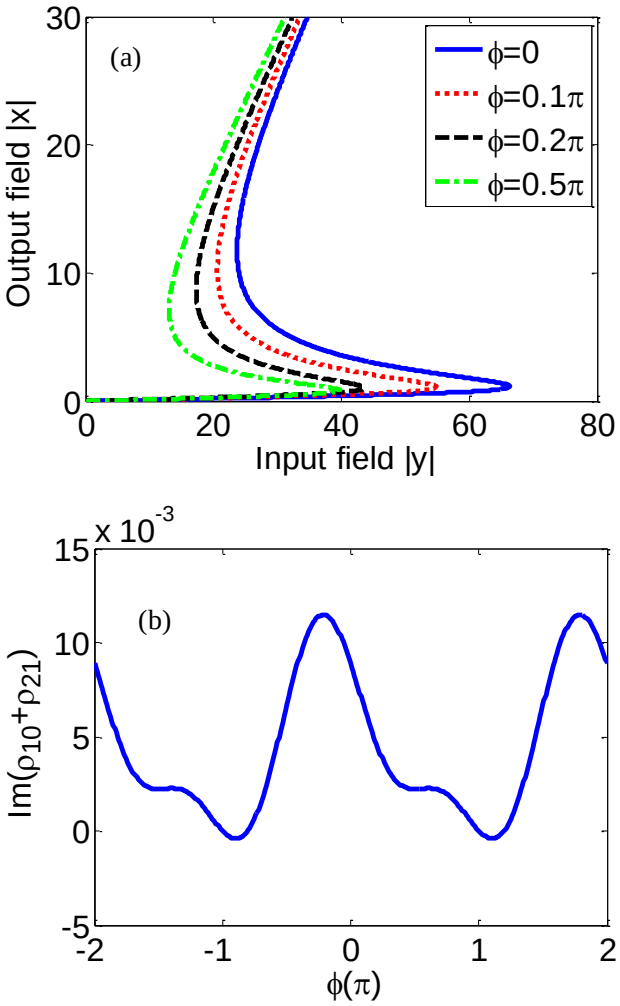

Fig. 8. Dependence of both OB and Im($\rho_{10}+\rho_{21}$) on the relative phase $\phi$of the applied fields. (a) OB behavior for different values of ϕ (b) Im($\rho_{10}+\rho_{21}$) as a function of ϕ with Ω_p=150. The other used parameters are $\Delta_p=\Delta_c=\Delta_d=0$, $\Omega_c=\Omega_d$=1, C=150

Finally, Fig. 8 shows the dependence of both OB and Im($\rho_{10}+\rho_{21}$) on the relative phase ϕ of the applied fields. When the relative phase of the applied fields increases, the threshold of OB goes down in Fig. 8 (a) for the absorption Im($\rho_{10}+\rho_{21}$) decreasing in Fig. 8 (b) between ϕ=0 and ϕ=0.5π.

Before ending this section, let us pay close attention to Ref. [27]. Wang et al. have also studied OB in a similar QWs system which can be controlled flexibly. Our system works in a different way relatively and can be regulated by second harmonic coupling field and another two fields via arranging carefully the corresponding parameters, which can be regarded as an available supplement study operating in a longer wavelength range.

4. Conclusions

To sum up, the optical bistable behaviors are investigated in two-coupled QWs. The system parameters such as the two coupling laser fields, the probe laser frequency detuning and the relative phase can be used to manipulate the OB. What is more, due to the flexibility of semiconductor QWs, the system is more practical than those in the atomic system, which can also be regulated effectively by the corresponding system parameters studied above. Our conclusions can also be extended to other wavelengths and systems with the same energy levels such as quantum dots. The results may be used to design new types optical switching.

Acknowledgements

This work is supported by the National Natural Science Foundation of China (Grant No. 11447182, 11447172 and 11547007), the Yangtze Fund for Youth Teams of Science and Technology Innovation (Grant No. 2015cqt03).

References

[1] D. F. Walls, P. Zoller, Opt. Commun. **34**(2), 260 (1980).
[2] W. Harshawardhan, G S. Agarwal, Phys. Rev. A **53**(3), 1812 (1996).
[3] A. Joshi, M. Xiao, Phys. Rev. Lett. **91**(14), 143904 (2003).
[4] A. Joshi, A. Brown, H. Wang, M. Xiao, Phys. Rev. A **67**(4), 041801(2003).
[5] A. Joshi, W. Yang, M. Xiao, Phys. Rev. A **68**(1), 015806 (2003).
[6] A. Joshi, W. Yang, M. Xiao, Phys. Lett. A **315**(3), 203 (2003).
[7] N. M. Litchinitser, I. R. Gabitov, A. I. Maimistov, Phys. Rev. Lett. **99**(11), 113902 (2007).
[8] J. H. Li, X.Y. Lü, J. M. Luo, Q. J. Huang, Phys. Rev. A **74**(3), 035801 (2006).
[9] Z. Wang, M. Xu, Opt. Commun. **282**(8), 1574 (2009).
[10] Z. H. Xiao, K. Kim, Opt. Commun. **283**(10), 2178 (2010).
[11] S. H. Asadpour, A. Eslami-Majd, J. Lumin. **132**(6), 1477 (2012).
[12] Z. Wang, A. X. Chen, Y. Bai, W. X. Yang, R. K. Lee, J. Opt. Soc. Am. B **29**(10), 2891 (2012).
[13] S. H. Asadpour, M. Jaberi, H. R. Soleimani, J. Opt. Soc. Am. B **30**(7), 1815 (2013).
[14] A. Jafari, R. Naderali, S. Bakkeshizadeh, Opt. Quantum Electron. **48**(1), 55 (2016).
[15] H. R. Hamedi, Laser Phys. **27**(6), 066002 (2017).
[16] A. A. Nejad, H. R. Askari, H. R. Baghshahi, Appl. Opt. **56**(10), 2816 (2017).
[17] Y. Y. Chen, Y. N. Li, R. G Wan, J. Opt. Soc. Am. B **35**(6), 1240 (2018).
[18] H. R. Hamedi, A. Khaledi-Nasab, A. Raheli, M. Sahrai, Optics Communications **312**, 117 (2014).
[19] X. Hu, H. Zhang, H. Sun, Y. Lei, H. Li, W. Liu, Applied Optics **55**(23), 6263 (2016).
[20] G Solookinejad, M. Payravi, M. Jabbari, M. Nafar, E. A. Sangachin, Laser Physics **27**(12), 125202 (2017).
[21] I. Karabulut, Superlattices and Microstructures **111**, 181 (2017).
[22] S. C. Tian, R. G Wan, C. Z. Tong, J. L. Zhang, X. N. Shan, X. H. Fu, Y. G Zeng, L. Qin, Y. Q. Ning, AIP Adv. **5**(6), 067144 (2015).
[23] S. Taherzadeh, R. Nasehi, M. Mahmoudi, Laser Physics **25**(4), 045901 (2015).
[24] J. Li, X. Hao, J. Liu, X. Yang, Phys. Lett. A **372**(5), 716 (2008).
[25] M. A. Antón, F. Carreño, O. G Calderón, S. Melle, Opt. Commun. **281**(12), 3301 (2008).
[26] J. Li, R. Yu, J. Liu, P. Huang, X. Yang, Physica E: Low-Dimens. Syst. Nanostruct. **41**(1), 70 (2008).
[27] Z. Wang, H. Fan, J. Lumin. **130**(11), 2084 (2010).
[28] Z. Wang, B. Yu, J. Opt. Soc. Am. B **30**(11), 2915 (2013).
[29] Z. Wang, S. Zhen, X. Wu, J. Zhu, Z. Cao, B. Yu, Opt. Commun. **304**, 7 (2013).
[30] A. Vafafard, S. Goharshenasan, N. Nozari, A. Mortezapour, M. Mahmoudi, J. Lumin. **134**, 900 (2013).
[31] S. C. Tian, R. G Wan, C. Z. Tong, Y. Q. Ning, J. Opt. Soc. Am. B **31**(11), 2681 (2014).
[32] H. R. Hamedi, Physica B **449**, 5 (2014).
[33] S. H. Asadpour, H. R. Soleimani, Physica B: Condens. Matter. **440**, 124 (2014).
[34] S. H. Asadpour, H. R. Soleimani, Opt. Commun. **315**, 347 (2014).
[35] A. Raheli, Brazilian Journal of Physics **48**(2), 111 (2018).
[36] Y. Chen, L. Deng, A. Chen, Annals of Physics **353**, 1 (2015).
[37] C. Yu, L. Sun, H. Zhang, F. Chen, IET Optoelectronics **12**(4), 215 (2018).
[38] H. R. Hamedi, M. R. Mehmannavaz, Laser Physics **25**(2), 025403 (2015).
[39] A. Golestani, A. Khaledi-Nasab, A. Asgari, Journal of Modern Optics **63**(6), 566 (2016).
[40] A. Joshi, Physical Review B **79**(11), 115315 (2009).

*Corresponding author: chchyu@yangtzeu.edu.cn